J Mol Model (2013) 19:239–245
DOI 10.1007/s00894-012-1537-6

ORIGINAL PAPER

Density functional investigation of CO adsorption on Ni-doped single-walled armchair (5,5) boron nitride nanotubes

Sarawut Tontapha · Vithaya Ruangpornvisuti · Banchob Wanno

Received: 25 May 2012 / Accepted: 12 July 2012 / Published online: 4 August 2012

Abstract The adsorption of CO onto Ni-doped boron nitride nanotubes (BNNTs) was investigated using density functional theory at the B3LYP/LanL2DZ level of theory. The structures of the Ni-doped BNNTs and their CO-adsorbed configurations were obtained. It was found that the strength of adsorption of CO onto Ni-doped perfect BNNTs is higher than that on defective BNNTs. The electronic properties of all of the adsorption configurations of CO on Ni-doped BNNTs are reported.

Keywords Adsorption · Boron nitride nanotubes · CO · Density functional theory · Ni-doped

Introduction

Nanomaterials with low weights and large specific surfaces have attracted increasing interest due to their potential applications, so their properties have been extensively studied. Carbon nanotubes (CNTs) were discovered by Iijima in 1991 [1], and since then, they have attracted much interest due to their outstanding properties. Boron nitride nanotubes (BNNTs) are one of a number of nanomaterials that have structures similar to CNTs [2, 3]. In comparison with CNTs, BNNTs have a wider band gap, higher chemical stability, excellent mechanical properties, and higher thermal conductivities [4, 5]. Single-, double-, triple-, and multiwalled BNNTs have been synthesized and identified [3, 6–8]. The structures of defective single-walled BNNTs [9, 10], as well as the doping [11, 12] and the functionalization [13, 14] of single-walled BNNTs and adsorption onto them [15–17] have been reviewed. The adsorption of small molecules (i.e., H_2, NO, N_2O, O_2, CO, CO_2, C_2H_4, C_2H_2, H_2O, NH_3) onto BNNTs and doped BNNTs were studied using density functional theory (DFT) [9, 18–23].

Carbon monoxide is a hazardous chemical that is produced by the incomplete burning of hydrocarbons. It is released in almost all combustion processes and is toxic, colorless, and odorless. Studying the adsorption of a toxic gas onto a surface material is of great interest. The molecular adsorption of CO onto a boron nitride nanocluster ($B_{12}N_{12}$) has been investigated using density functional theory [24]. It was found that CO adsorption can induce significant changes in the cluster's electronic properties, suggesting that this $B_{12}N_{12}$ cluster is a potential sensor for CO detection.

Generally, defects in BNNT defects are either B or N vacancies, square/octagon pair defects, doping agents, or Stone–Wales (SW) defects. SW defects which are generated by rotating the B–N bond by 90°, meaning that four associated hexagons fuse into two pentagon/heptagon pairs, have been widely studied. Note that there are two possible SW defects—straight SW and slanted SW defects—according to the orientation of the rotated B–N bond. Also, the geometries, electronic properties, relative stabilities, and reactivities of BNNTs with SW defects have been reported by Li and coworkers [10]. They showed that the reactivity of SW defect site is higher than that of a perfect site. Moreover, the adsorption of Ni onto single-walled BNNTs with intrinsic defects has been studied using DFT calculations, and the

Electronic supplementary material The online version of this article (doi:10.1007/s00894-012-1537-6) contains supplementary material, which is available to authorized users.

S. Tontapha · B. Wanno (✉)
Center of Excellence for Innovation in Chemistry and Department of Chemistry, Faculty of Science, Mahasarakham University, Maha Sarakham 44150, Thailand
e-mail: banchobw@gmail.com

V. Ruangpornvisuti
Department of Chemistry, Faculty of Science, Chulalongkorn University, Bangkok 10330, Thailand

results of that study were reported by Zhao and coworkers [25]. They found that the existence of defects in BNNTs clearly improves the chemical reactivity associated with Ni adsorption. In addition, the charge transfer, band gap, and density of states of Ni adsorbed onto BNNTs have been reported.

In the work described in the present paper, we investigated the configurations of CO that is adsorbed onto Ni-doped BNNTs and the electronic properties of these configurations using density functional theory with B3LYP/LanL2DZ computations. The frontier molecular orbital energies, energy gaps, adsorption energies, partial charge transfers, and geometric parameters of the CO adsorbed onto Ni-doped BNNTs were determined.

Computational details

We selected seven-layered armchair (5,5) BNNTs for study. All of the atoms at both ends of the BNNTs were terminated with hydrogen atoms. All of these hydrogen-terminated BNNT structures therefore had the same chemical formula, $B_{35}N_{35}H_{20}$. The (5,5) BNNT models were categorized into three types: "perfect site" (PS) BNNT (i.e., with no defects); BNNT with straight Stone–Wales defects (SW1); BNNT with slanted Stone–Wales defects (SW2). For the Ni-doped BNNT structures, an Ni atom was added to the outer side wall of each type (perfect and defective) of BNNT approximately midway along the tube length. This procedure allowed us to create structures for perfect and Stone–Wales defective BNNTs doped with an Ni atom at the particular adsorption site of each BNNT. As displayed in Fig. 1, we denoted the chemical bonds in the vicinity of the adsorption site as follows: "D" for a diagonal B–N bond and "O" for an orthogonal B–N bond in the PS structure; "Z_B" for a zigzag B–B bond, "A" for an axial B–N bond, and "Z_N" for a zigzag N–N bond in the SW1 structure; and "Z_B" for a zigzag B–B bond, "A" for an axial B–N bond, and "Z_N" for a zigzag N–N bond in the SW2 structure [26].

The adsorption of carbon monoxide onto these BNNTs doped with Ni was investigated. All geometry optimization performed in the present study was carried out using density functional theory. The hybrid functional B3LYP, Becke's three-parameter exchange functional [27], and the Lee–Yang–Parr correlation functional [28] were employed. The LanL2DZ [29–31] basis set (Dunning/Huzinaga valence double-zeta for first-row elements, and Los Alamos effective core potentials (ECP) plus double-zeta for heavier elements) was also used. All calculations were performed using the program GAUSSIAN 03 [32]. The most stable structure obtained from the geometric optimization of each system was used in the final single-point energy calculations. Electronic properties, including the energy gap (E_{gap}) between the highest occupied molecular orbital (HOMO) and the lowest unoccupied molecular orbital (LUMO), the partial charge transfer (PCT) upon the adsorption of CO, and the density of states (DOS), were studied. DOS plots for all of the BNNTs and their possible Ni-doped structures as well as their CO-adsorbed configurations were derived from the orbital energies present in the Gaussian output file, and were simulated using the program GaussSum 2.2 [33]. The adsorption energies (ΔE_{ads}) of a CO molecule onto the Ni in the Ni-doped perfect and Stone–Wales defective BNNTs were calculated according to the following equation:

$$\Delta E_{ads} = E_{CO/Ni-BNNT} - (E_{Ni-BNNT} + E_{CO}) \quad (1)$$

where $E_{CO/Ni\text{-}BNNT}$ and $E_{Ni\text{-}BNNT}$ are the total energy of the Ni-doped BNNT with CO adsorbed onto it and the total energy of the Ni-doped BNNT, respectively. E_{CO} is the total energy of a CO molecule.

Basis set superposition error (BSSE) corrections for the adsorption energies were realized at the same level of theory using Boys–Bernardi counterpoise (CP) calculations [34–37]. Here, the adsorption energy corrected for the BSSE correction is denoted ΔE_{ads}^{BSSE}.

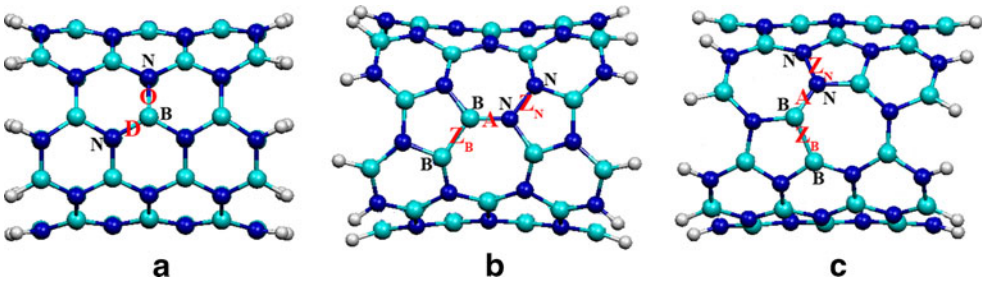

Fig. 1 **a**–**c** Side walls of the modeled **a** PS, **b** SW1, and **c** SW2 BNNT structures. Adsorption sites that are doped with Ni are labeled according to the nearest chemical bond: **a** "D" for a diagonal B–N bond and "O" for an orthogonal B–N bond in the PS structure; **b** "Z_B" for a zigzag B–B bond, "A" for an axial B–N bond, and "Z_N" for a zigzag N–N bond in the SW1 structure; **c** "Z_B" for a zigzag B–B bond, "A" for an axial B–N bond, and "Z_N" for a zigzag N–N bond in the SW2 structure [26]

Results and discussion

Structural properties

In our previous study, we investigated and reported the geometries and stabilities of armchair (5,5) BNNTs doped with Ni, Pd, and Pt atoms [26]. The The B3LYP/LanL2DZ-optimized structures of perfect and defective BNNTs (PS-BNNT, SW1-BNNT, SW2-BNNT; see definitions above) as well as their Ni-, Pd-, and Pt-doped structures were calculated. The relative energies, frontier molecular orbital energies, energy gaps, and chemical indices of all of the perfect and defective BNNTs and their Ni-, Pd-, and Pt-doped structures were also studied. The results showed that the BNNTs show the strongest binding to Ni among the three dopant metals. Thus, in the present work, we chose to study the adsorption of CO onto Ni-doped BNNTs.

Therefore, we obtained all possible adsorption configurations for CO on the Ni-doped perfect and defective BNNTs (Ni-PS, Ni-SW1, and Ni-SW2). When the CO is adsorbed onto Ni-PS, Ni-SW1, and Ni-SW2, it may do so by pointing either its C or its O atom toward the side-wall atoms of the BNNT; we denote these orientations by CO and CO, respectively. Therefore, the adsorption configurations in which CO points its C atom toward the side-wall atoms of each BNNT are denoted CO/Ni-PS, CO/Ni-SW1, and CO/Ni-SW2. Correspondingly, those in which the O atom of CO points toward the side-wall atoms are then termed CO/Ni-PS, CO/Ni-SW1, and CO/Ni-SW2.

The B3LYP/LanL2DZ-optimized structures of the Ni-doped PS, SW1, and SW2 BNNTs with a CO adsorbed onto them are displayed in Figs. 2, 3, and 4, respectively. Selected bond distances in these structures are listed in Table 1. The calculated Ni–CO distances are 1.708–1.829 and 1.805–2.027 Å for the CO-adsorbed configurations with CO and CO, respectively, which are much shorter than the van der Waals distances for BNNTs with adsorbed CO reported in [9]. The average C–O bond length in the CO molecule when it has been adsorbed onto these BNNTs is about 1.179 Å, while the C–O bond length of the free CO molecule is 1.166 Å. Interestingly, for the CO/Ni-SW1 configuration, the Ni atom is located above the B–N bond at the Z_B site after adsorption (see Fig. 3e).

Adsorption energy

The energies associated with the adsorption of CO onto the Ni-doped PS, SW1, and SW2 BNNTs, computed at the B3LYP/LanL2DZ level with and without the BSSE correction, as well as the frontier molecular orbital energies, energy gaps, and the partial charge transfer values of the corresponding CO-adsorbed configurations are shown in Table 2. These adsorption energies indicate that CO adsorption by the Ni-doped BNNTs is always an exothermic process. In addition, the calculated results show that adsorption via the CO orientation leads to a stronger interaction than adsorption via the CO orientation. The binding strengths

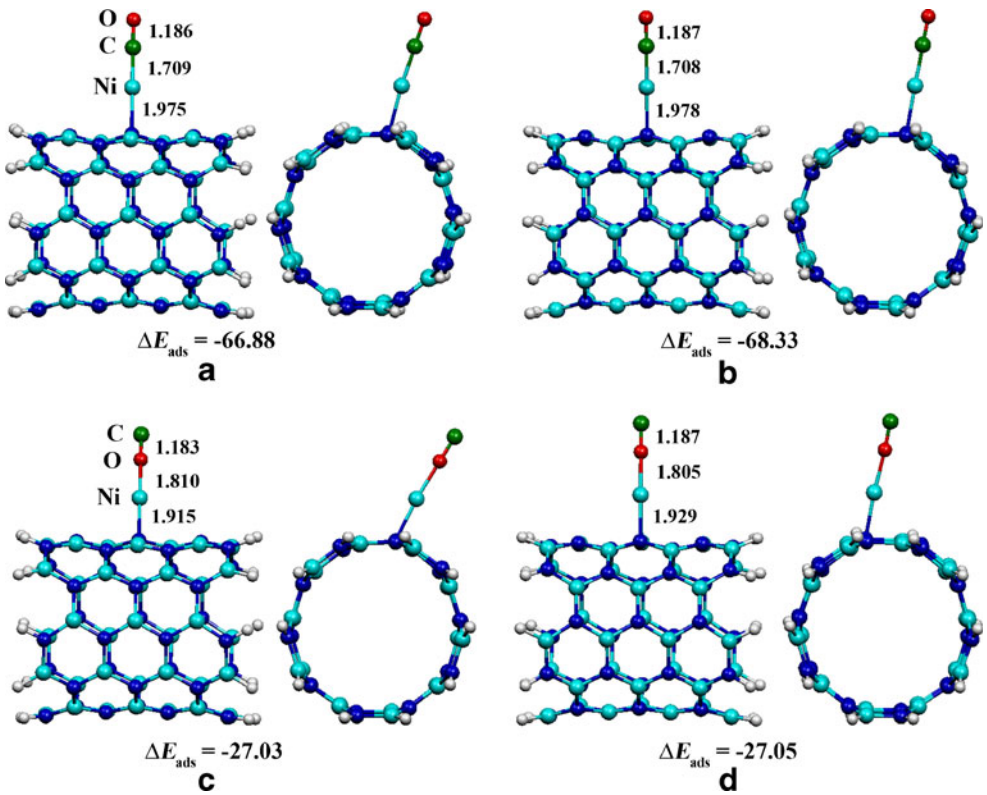

Fig. 2 **a**–**d** The B3LYP/LanL2DZ-optimized structures for CO adsorbed onto the Ni-doped PS BNNT: **a** CO/Ni-PS at the D site, **b** CO/Ni-PS at the O site, **c** CO/Ni-PS at the D site, and **d** CO/Ni-PS at the O site. In each case, the *left and right diagrams* show side and front views of the nanotubes. Bond distances and adsorption energies are in Å and kcal mol^{-1}, respectively

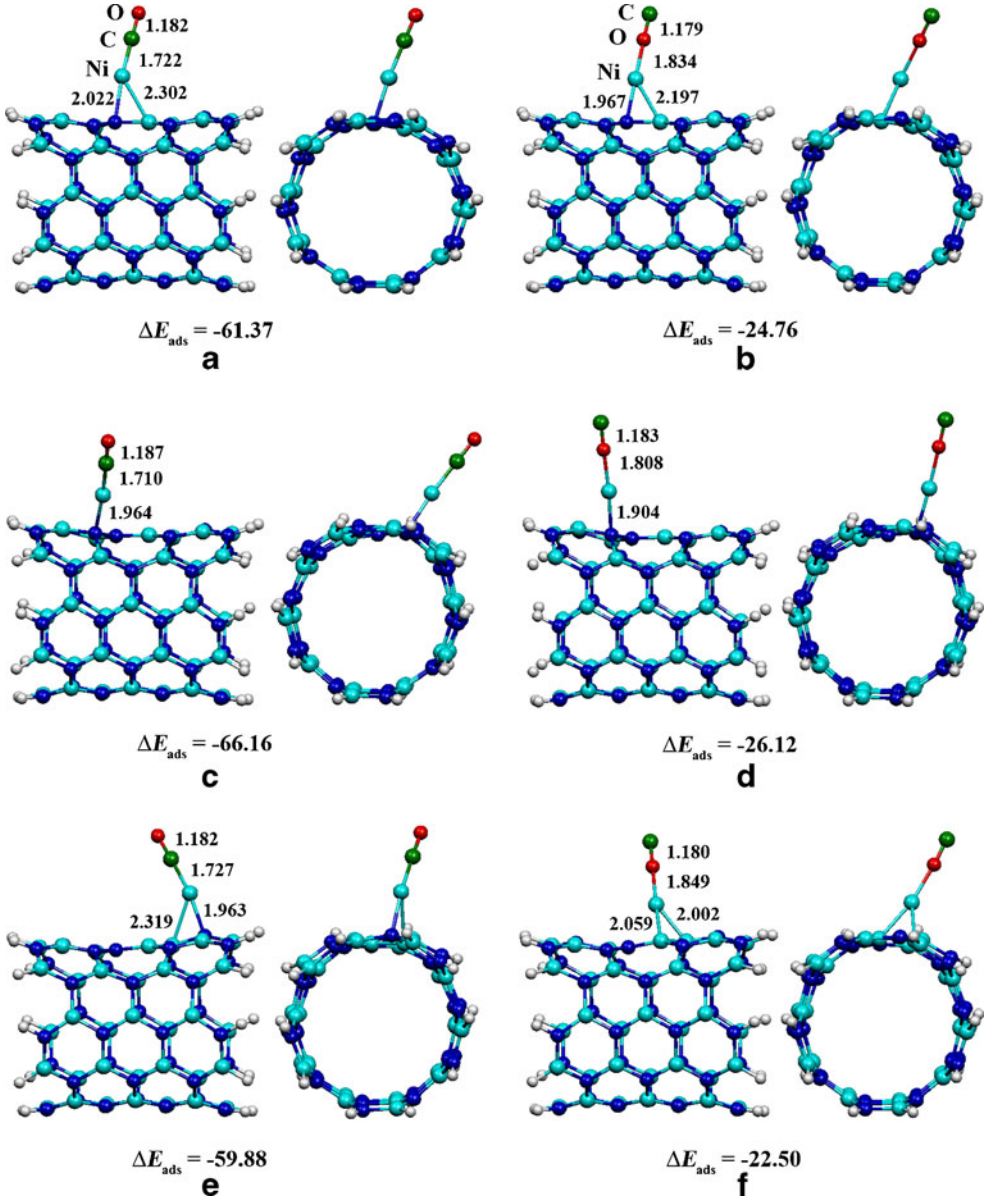

Fig. 3 **a**–**f** The B3LYP/LanL2DZ-optimized structures for CO adsorbed onto the Ni-doped SW1 BNNT: **a** CO/Ni-SW1 at the A site, **b** CO/Ni-SW1 at the A site, **c** CO/Ni-SW1 at the Z_N site, **d** CO/Ni-SW1 at the Z_N site, **e** CO/Ni-SW1 at the Z_B site, and **f** CO/Ni-SW1 at the Z_B site. In each case, the *left and right diagrams* show side and front views of the nanotubes. Bond distances and adsorption energies are in Å and kcal mol^{-1}, respectively

associated with the adsorption of CO at the different sites on the Ni-doped BNNTs, obtained with and without the BSSE correction, are reported in Table 2. Based on those calculated results, the Ni-doped BNNTs show strong binding with CO molecule; the highest values of the adsorption energy ΔE_{ads} and ΔE_{ads}^{BSSE} are −68.33 and −60.24 kcal mol^{-1}, respectively, which were obtained with the CO/Ni-PS configuration where binding occurs at the O site. In this case, the adsorption is accompanied by −0.108 *e* of PCT from BNNT to CO, which occurs due to the strong electronegativity of the O atom of the CO molecule. On the other hand, the binding of CO to the Ni-doped SW2 BNNT is the weakest among the configurations investigated, with an estimated ΔE_{ads} of −12.70 kcal mol^{-1} and a ΔE_{ads}^{BSSE} of −7.36 kcal mol^{-1}, indicating that CO adsorption onto this Ni-doped defective BNNT is not very favorable. The BSSE values for CO adsorption onto the studied surfaces are rather low: 5.34–8.24 kcal mol^{-1}. The adsorption of CO onto the Ni-doped BNNTs is much more favorable that the absorption of CO onto pure BNNTs and chemical-doped BNNTs (as reported in [9, 38]). It is interesting to note that the BNNTs with PS and SW defects show different reactivities toward CO adsorption. This interaction can be described as molecular chemisorption as it is highly exothermic.

Frontier orbitals and energy gaps

The frontier orbitals and energy gaps for the adsorption of a CO molecule by Ni-doped PS, SW1, and SW2 BNNTs, as obtained using B3LYP/LanL2DZ, are listed in Table 2. The energy gaps (E_{gap}) of Ni-doped PS-BNNT, SW1-BNNT, and SW2-BNNT are 2.75–3.62 eV, which are much lower

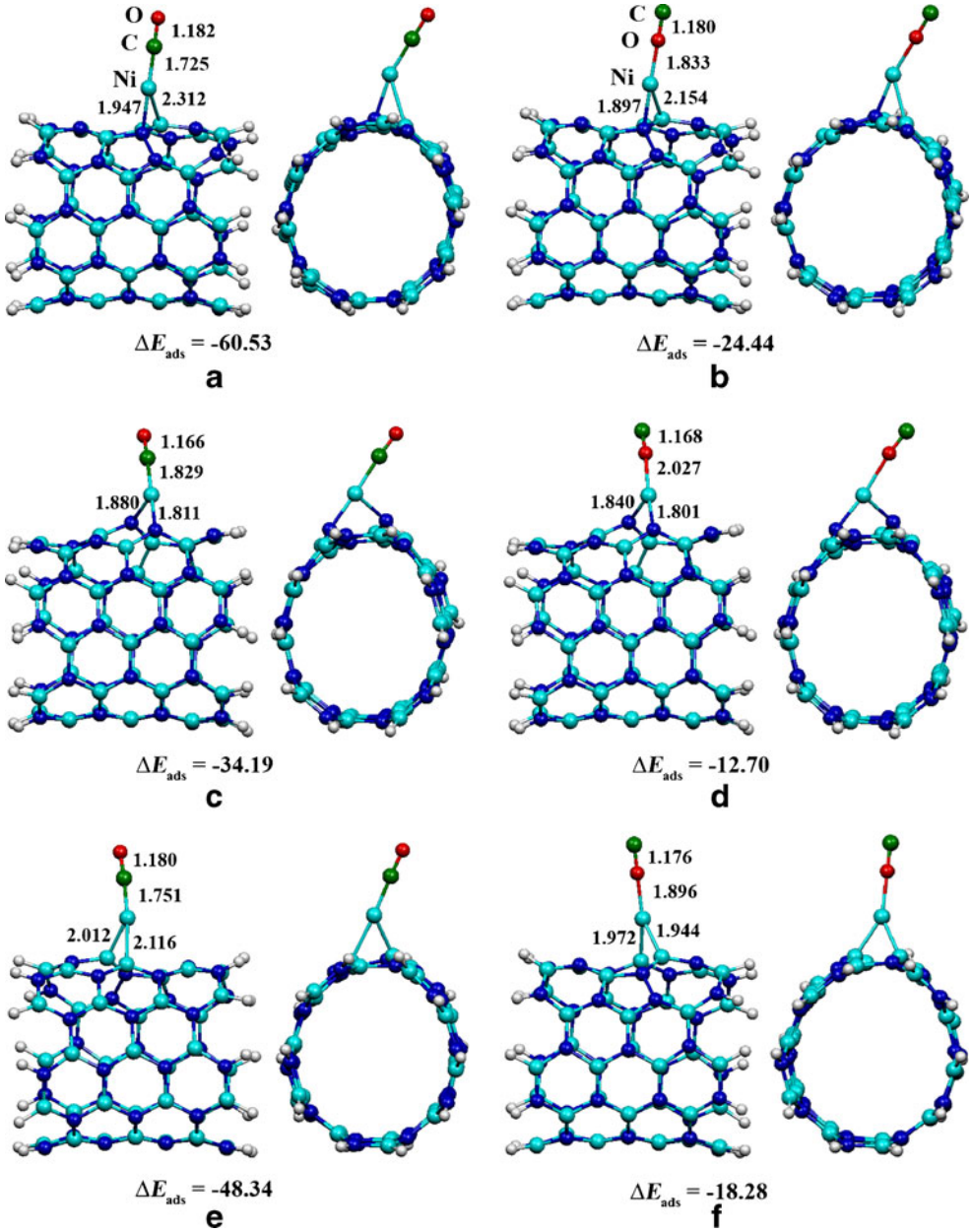

Fig. 4 **a**–**f** The B3LYP/LanL2DZ-optimized structures for CO adsorbed onto the Ni-doped SW2 BNNT: **a** CO/Ni-SW2 at the A site, **b** CO/Ni-SW2 at the A site, **c** CO/Ni-SW2 at the Z_N site, **d** CO/Ni-SW2 at the Z_N site, **e** CO/Ni-SW2 at the Z_B site, and **f** CO/Ni-SW2 at the Z_B site. In each case, the *left and right diagrams* show side and front views of the nanotubes. Bond distances and adsorption energies are in Å and kcal mol^{-1}, respectively

than those of the corresponding undoped nanotubes (see our previous work [26]; the energy gaps for the undoped PS-BNNT, SW1-BNNT, and SW2-BNNT are 6.10, 5.20, and 4.79 eV, respectively). The frontier orbitals of the Ni-doped PS, SW1, and SW2 BNNTs with CO adsorbed onto them are displayed in Figs. S1, S2, and S3 of the "Electronic supplementary material" (ESM), respectively. The frontier orbitals show that the HOMO orbitals of all of these complexes are located in the vicinity of the Ni dopant, while the LUMO orbitals are located around the CO, indicating that Ni transfers electrons to the CO molecule. These results confirm that the CO molecule forms strong complexes with Ni-doped BNNTs.

Partial charge transfer

Values for the partial charge transfer (PCT), defined as the charge transfer from the CO molecule to the atom in the Ni-doped BNNT to which it binds (in other words, as the difference between the charge on the CO molecule when has been adsorbed onto the Ni-doped BNNT and the charge on the isolated CO molecule), were obtained using natural bond orbital analysis. The calculated partial charge transfer values are listed in Table 2. The results show that for most of the CO-adsorbed configurations, the PCTs are negative, indicating that charge is transferred from the Ni-doped BNNT to the CO molecule when it is adsorbed. There are, however, two exceptions to this rule: the configuations CO/

Table 1 C–O bond lengths and CO adsorption distances (i.e., between CO and the Ni atom, in Å) in the Ni-doped PS, SW1, and SW2 BNNTs with CO adsorbed onto them, as shown in Figs. 2, 3, and 4

Molecular species	Site	Ni–X distance	C–O bond length
PS system:			
CO/Ni-PS	D	1.709 [a]	1.186
CO/Ni-PS	D	1.810 [b]	1.183
CO/Ni-PS	O	1.708 [a]	1.187
CO/Ni-PS	O	1.805 [b]	1.183
SW1 system:			
CO/Ni-SW1	A	1.722 [a]	1.182
CO/Ni-SW1	A	1.834 [b]	1.179
CO/Ni-SW1	Z_N	1.710 [a]	1.187
CO/Ni-SW1	Z_N	1.808 [b]	1.183
CO/Ni-SW1	Z_B	1.727 [a]	1.182
CO/Ni-SW1	Z_B	1.849 [b]	1.180
SW2 system:			
CO/Ni-SW2	A	1.725 [a]	1.182
CO/Ni-SW2	A	1.833 [b]	1.180
CO/Ni-SW2	Z_N	1.829 [a]	1.166
CO/Ni-SW2	Z_N	2.027 [b]	1.168
CO/Ni-SW2	Z_B	1.751 [a]	1.180
CO/Ni-SW2	Z_B	1.896 [b]	1.176
CO		–	1.166

[a] X=C

[b] X=O

Ni-SW2 (at Z_N site) and CO/Ni-SW2 (at Z_N site), for which the PCT values are positive.

Density of states (DOS)

The B3LYP/LanL2DZ-computed values for the electronic density of states of Ni-doped PS, SW1, and SW2 BNNTs with CO adsorbed onto them are plotted in Figs. S4, S5, and S6 in the ESM, respectively. The Fermi level (E_F) values observed in the present work are in the range −3.129 to −4.919 eV, which indicates that the DOS at around the Fermi level for each Ni-doped BNNT with CO adsorbed onto it is slightly different from that of the Ni-doped BNNT (i.e., without CO adsorbed). Interestingly, Figs. S6e and S6h show that the Fermi levels of the CO-adsorbed configurations are significantly different from those of other complexes, indicating that CO adsorption generates an impurity state near the conduction band.

Conclusions

The structures of the adsorption configurations of Ni-doped BNNTs with CO adsorbed onto them were obtained using B3LYP/LanL2DZ. Seven-layered armchair (5,5) BNNTs were selected for study, and all of the atoms at each end were terminated with hydrogen atoms, giving all of them a chemical formula of $B_{35}N_{35}H_{20}$. The adsorption energies for the adsorption of CO by Ni-doped BNNTs were in the range −68.33 to

Table 2 Energies associated with the adsorption of CO onto the Ni-doped PS, SW1, and SW2 BNNT structures, as well as the frontier molecular orbital energies, energy gaps, and the partial charge transfer values of the corresponding CO-adsorbed configurations

Complexes	Site	ΔE_{ads} [a]	BSSE [a]	Δ[a]	E_{HOMO} [b]	E_{LUMO} [b]	E_{gap} [b]	PCT [c]
PS system:								
CO/Ni-PS	D	−66.88	8.09	−58.79	−5.290	−1.073	4.216	−0.102
CO/Ni-PS	D	−27.03	5.60	−21.43	−4.941	−1.717	3.224	−0.089
CO/Ni-PS	O	−68.33	8.09	−60.24	−5.241	−1.071	4.170	−0.108
CO/Ni-PS	O	−27.05	5.54	−21.51	−4.680	−1.551	3.129	−0.110
SW1 system:								
CO/Ni-SW1	A	−61.37	8.24	−53.13	−5.504	−1.781	3.723	−0.075
CO/Ni-SW1	A	−24.76	5.80	−18.96	−5.051	−2.106	2.946	−0.100
CO/Ni-SW1	Z_N	−66.16	8.15	−58.01	−5.189	−1.297	3.892	−0.109
CO/Ni-SW1	Z_N	−26.12	5.52	−20.60	−4.746	−1.695	3.051	−0.100
CO/Ni-SW1	Z_B	−59.88	8.09	−51.79	−5.577	−1.807	3.770	−0.075
CO/Ni-SW1	Z_B	−22.50	5.87	−16.63	−5.101	−2.018	3.083	−0.071
SW2 system:								
CO/Ni-SW2	A	−60.53	8.15	−52.38	−5.661	−1.945	3.716	−0.075
CO/Ni-SW2	A	−24.44	5.54	−18.90	−5.214	−2.114	3.100	−0.060
CO/Ni-SW2	Z_N	−34.19	7.79	−26.40	−6.461	−3.376	3.086	0.026
CO/Ni-SW2	Z_N	−12.70	5.34	−7.36	−6.275	−3.053	3.221	0.030
CO/Ni-SW2	Z_B	−48.34	7.95	−40.39	−5.687	−1.884	3.803	−0.069
CO/Ni-SW2	Z_B	−18.28	5.72	−12.56	−5.146	−2.404	2.742	−0.034

[a] In kcal mol^{-1}

[b] In eV

[c] In *e*

−12.70 kcal mol^{-1}. The energy gaps for the Ni-doped BNNTs with CO adsorbed onto them, derived using B3LYP/LanL2DZ, were 2.742–4.216 eV. The highest binding strength of CO to the Ni-doped BNNT was noted for the CO/Ni-PS configuration with binding at the "O" site (ΔE_{ads}=−68.33 kcal mol^{-1}), which was associated with a large amount of charge transfer.

Acknowledgments Financial support from the Center for Innovation in Chemistry (PERCH-CIC), Commission on Higher Education, Ministry of Education to Sarawut Tontapha is gratefully acknowledged, as is the financial support (grant no. MRG5180141) provided by the Thailand Research Fund to Banchob Wanno. We also thank the Supramolecular Chemistry Research Unit, Department of Chemistry, Faculty of Science, Mahasarakham University, for allowing us to use their facilities.

References

1. Iijima S (1991) Nature 354:56–58
2. Rubio A, Corkill JL, Cohen ML (1994) Phys Rev B 49:5081–5084
3. Chopra NG, Luyken RJ, Cherrey K, Crespi VH, Cohen ML, Louie SG, Zettl A (1995) Science 269:966–967
4. Golberg D, Bando Y, Huang Y, Terao T, Mitome M, Tang C, Zhi C (2010) ACS NANO 4:2979–2993
5. Zhi C, Bando Y, Tang C, Golberg D (2010) Mater Sci Eng R 70:92–111
6. Wang J, Kayastha VK, Yap YK, Fan Z, Lu JG, Pan Z, Ivanov IN, Puretzky AA, Geohegan DB (2005) Nano Lett 5:2528–2532
7. Kim MJ, Chatterjee S, Kim SM, Stach EA, Bradley MG, Pender MJ, Sneddon LG, Maruyama B (2008) Nano Lett 8:3298–3302
8. Arenal R, Stephan O, Kociak MD, Taverna AL, Colliex C (2005) Phys Rev Lett 95:127601–127605
9. An W, Wu X, Yang JL, Zeng XC (2007) J Phys Chem C 111:14105–14112
10. Li Y, Zhou Z, Golberg D, Bando Y, Schleyer PR, Chen Z (2008) J Phys Chem C 112:1365–1370
11. He KH, Zheng G, Chen G, Wan M, Ji GF (2008) Physica B 403:4213–4216
12. Kim G, Park J, Hong S (2012) Chem Phys Lett 522:79–82
13. Wu X, An W, Zeng XC (2006) J Am Chem Soc 128:12001–12006
14. Wang R, Zhu R, Zhang D (2008) Chem Phys Lett 467:131–135
15. Chen YK, Liu LV, Wang YA (2010) J Phys Chem C 114:12382–12388
16. Zheng JW, Zhang LP, Wu P (2010) J Phys Chem C 114:5792–5797
17. Zhang JM, Wang SF, Chen LY, Xu KW, Ji V (2010) Eur Phys J B 76:289–299
18. Baei MT (2012) Monatsh Chem 143:989–995. doi:10.1007/s00706-011-0680-6
19. Choi H, Park YC, Kim YH, Sup Y (2011) J Am Chem Soc 133:2084–2087
20. Xie Y, Huo YP, Zhang JM (2012) Appl Surf Sci 258:6391–6397
21. Li XM, Tian WQ, Huang XR, Sun CC, Jiang L (2009) J Mol Struct (THEOCHEM) 901:103–109
22. Dong Q, Li XM, Tian WQ, Huang XR, Sun CC (2010) J Mol Struct (THEOCHEM) 948:83–92
23. Baei MT, Soltani AR, Moradi AV, Lemeski ET (2011) Comput Theor Chem 970:30–35
24. Beheshtian J, Bagheri Z, Kamfiroozi M, Ahmadi A (2011) Microelectron J 42:1400–1403
25. Zhao JX, Ding YH (2008) J Phys Chem C 112:5778–5783
26. Tontapha S, Morakot N, Ruangpornvisuti V, Wanno B (2012) Struct Chem. doi:10.1007/s11224-012-9988-z
27. Becke AD (1993) J Chem Phys 98:5648–5652
28. Lee C, Yang W, Parr RG (1988) Phys Rev B 37:785–789
29. Hay PJ, Wadt WR (1985) J Chem Phys 82:270–283
30. Wadt WR, Hay PJ (1985) J Chem Phys 82:284–298
31. Hay PJ, Wadt WR (1985) J Chem Phys 82:299–310
32. Frisch MJ, Trucks GW, Schlegel HB, Scuseria GE, Robb MA, Cheeseman JR, Montgomery JA, Vreven T, Kudin KN, Burant JC, Millam JM, Iyengar SS, Tomasi J, Barone V, Mennucci B, Cossi M, Scalmani G, Rega N, Petersson GA, Nakatsuji H, Hada M, Ehara M, Toyota K, Fukuda R, Hasegawa J, Ishida M, Nakajima T, Honda Y, Kitao O, Nakai H, Klene M, Knox JE, Hratchian HP, Cross JB, Adamo C, Jaramillo J, Gomperts R, Stratmann RE, Yazyev O, Austin AJ, Cammi R, Pomelli C, Ochterski JW, Ayala PY, Morokuma K, Voth GA, Salvador P, Dannenberg JJ, Zakrzewski VG, Dapprich S, Daniels AD, Strain MC, Farkas O, Malick DK, Rabuck AD, Raghavachari K, Foresman JB, Ortiz JV, Cui Q, Baboul AG, Clifford S, Cioslowski J, Stefanov BB, Liu G, Liashenko A, Piskorz P, Komaromi I, Martin RL, Fox DJ, Keith T, Laham MA A, Peng CY, Nanayakkara A, Challacombe M, Gill PMW, Johnson B, Chen W, Wong MW, Gonzalez C, Pople JA (2008) Gaussian 03, revision E.01. Gaussian Inc., Wallingford
33. O'Boyle NM, Tenderholt AL, Langner KM (2008) J Comput Chem 29:839–845
34. Boys SF, Bernadi F (1970) Mol Phys 19:553–566
35. Mayer I, Surjan PR (1992) Chem Phys Lett 191:497–499
36. Turi L, Dannenberg JJ (1993) J Phys Chem 97:2488–2490
37. Makowski M, Raczyska ED, Chmurzyski L (2001) J Phys Chem A 105:869–874
38. Baierle RJ, Schmidt TM, Fazzio A (2007) Solid State Commun 142:49–53